

ESR, IR and Optical Absorption Studies of Co^{2+} ions in ZnO-PbO- B_2O_3 glass System.

M. Farouk

Physics department, Faculty of science, Al Azhar University, Nasr City,
Cairo 11884, Egypt.
mf_egypt22375@yahoo.com

Glassy system of composition $x \text{Co}_2\text{O}_3$ -(40-x) ZnO-10PbO-50 B_2O_3 , (where $x = 0, 0.1, 0.3, 0.5$ and 1 mol %) were prepared by conventional melt-quenching technique. The X-Ray Diffraction pattern of the glass samples shows no sharp peaks, indicating the amorphous nature. FT-IR spectra of the glasses show vibration modes corresponding to stretching of BO_3 trigonal, BO_4 tetrahedral units and of B-O-B bending bonds. The observed red shift of optical absorption edge (UV cutoff) show monotonous decrease in indirect optical band gap energy (E_{opt}) by increasing Co_2O_3 content in the glasses based on their absorption spectra. Absorption spectra of ZLB: Co^{2+} have exhibited two tetrahedral bands corresponding to (${}^4\text{T}_{1g}(\text{F}) \rightarrow {}^4\text{T}_{1g}(\text{P})$) and (${}^4\text{T}_{1g}(\text{F}) \rightarrow {}^4\text{A}_{2g}(\text{F})$) transitions and an octahedral band in (${}^4\text{T}_{1g}(\text{F}) \rightarrow {}^2\text{T}_{1g}(\text{D})$) transition. ESR spectra exhibit characteristic resonance signals of Co^{2+} ions and a well resolved six line hyperfine structure.

1. Introduction:

Recently, heavy-metal oxide (HMO) glasses based on large atomic weight cations have attracted enhanced interest because of their peculiar encouraging and important optical properties. The HMO based glasses are characterized by high density, and high refractive index. They are identified as electro-optic materials and are used as electro-optic switches, solid-state laser materials and applications [1-5]. Regarding transition metal ions doped materials, only a little work has so far been reported [6-8]. Glass color is an essential factor in both glass making technology and glass state science.

The color depends on the electron transition as well as on the chemical composition. This is based on the fact that splitting energy term in 3d metals is

strongly affected by ligands [9].

Amorphous and crystalline lead borates belong to the attractive solid-state materials from the structural and optical points of view. Lead borate glasses are extensively studied in recent years due to their wide glass-forming region and quite an easy preparation, high chemical stability, and UV–VIS–NIR light transmittance, presence of structurally different borate units are the most important and advantageous points of PbO-B₂O₃ systems.

Additionally, lead borate glass is promising host for incorporation of transition metals and rare earth ions [1, 10-13]. Earlier workers conducted optical studies on lead zinc borate glasses and noticed a long infrared cutoff as a property that shows their usefulness in many potential applications [14]. ZnO-B₂O₃ glasses are well known due to their wide applications in plasma display panels for high quality performance. These glasses possess high insulating strength, low thermal expansion coefficient and good transparency over a wide of wave-length range [15, 16]. ZnO enters in the glass structure in the form of both network former and network modifier. CoO, an anti-ferromagnetic material, is more stable in the natural environment. When it is incorporated in a host system, it improves the sintering behavior of the system which could have a wide range of applications in various industrial sectors [17].

Normally cobalt ions exist in Co²⁺ state; however, under extreme conditions in the alkaline rich glasses it can exist in Co³⁺ state, both Co²⁺ and Co³⁺ ions occupy tetrahedral as well as octahedral sites in the glass matrices. Co²⁺ ions create color centers with absorption bands in the visible and NIR regions [18]. Co²⁺ ion exhibits a strong colorant features, which produces an intense blue color in glasses under tetrahedral symmetry. However, its color shade changes to pink under octahedral symmetry [1,19,20]. UV/VIS spectroscopy is a simple and most commonly experimental technique used for study of colored glasses and determination of valences and co-ordination of transition metals in glasses [9]. In the present study of ESR spectroscopy was used beside optical absorption spectra for sake of comparison.

2. Experimental:

The starting materials used in the present work were reagent grade of H₃BO₃, ZnO, PbO and Co₂O₃. The host glass composition is taken as x Co₂O₃-(40-x) ZnO-10PbO-50B₂O₃, where x = 0, 0.1, 0.3, 0.5 and 1 mol%. All weighted chemicals were powdered finally and mixed thoroughly. Each batch was melted in ceramic crucibles in an electrical furnace at 1000°C for an hour.

The melts were quenched in between two brass plates to produce discs of about 0.2 cm thickness. The undoped glasses have been found to be colorless, and the Co^{2+} ions doped glass show the prominent dark blue with higher Co_2O_3 concentration. The glass composition here is named ZLB (zinc lead borate) glass system. X-ray diffraction (XRD) spectra were obtained on a Shimadzu XD3A diffractometer. Glass densities were measured with toluene as an immersion solvent using the Archimedes's principle. Infrared absorption spectra were recorded using FTIR (PerkinElmer) in the range (1700–400 cm^{-1}), the sample powder was mixed with KBr of high purity. The optical absorption spectra of polished glass samples were taken on JASCO V670 spectrophotometer in the region of 190–1100 nm. The ESR spectra were recorded at room temperature on ESR spectrometer (EMX-Bruker) operating in X-band frequency.

3. Results and Discussion:

3. 1. X-ray Diffraction and Physical Properties:

Fig. (1) Shows the typical X-ray diffraction patterns of pure (zero cobalt) and 1 mol % Co_2O_3 doped ZLB glasses. The XRD pattern of the glass samples shows no sharp peaks, which is a sign of amorphous material. Composition of the glasses, density (ρ), Molar volume (V_m) and cobalt ion concentration (N) listed in Table (1). The ion concentration (N) and interionic distance (r_i), were calculated using the relation [21]:

$$N(\text{ion}/\text{cm}^3) = \frac{x\rho N_A}{M_W} \quad (1)$$

$$r_i(\text{Å}^0) = \left(\frac{1}{N}\right)^{1/3} \quad (2)$$

and a polaron radius (r_p) using the relation :

$$r_p(\text{Å}^0) = (1/2)(\pi/6N)^{1/3} \quad (3)$$

The values are also listed in Table (1). The density is a powerful tool, capable of studying the changes in the structure of glasses. It depends on compactness, geometrical configurations, co-ordination numbers, cross-link densities, and dimensions of interstitial spaces of the glass [22]. Fig. (2), shows the dependence of density and molar volume on cobalt oxide (Co_2O_3) content. The obtained results reveal that the density decreases from 3.84 to 3.68 g/cm^3 , and the molar volume increases from 30.37 to 31.86 cm^3/mol as the Co_2O_3

content increases at the expense of the ZnO content. ZnO is in general glass modifier and enters the glass network by breaking up the B-O-B bonds (normally the oxygen's of ZnO break the local symmetry while Zn^{2+} ions occupy interstitial positions) and introduces co-ordinate defects known as dangling bonds along with non-bridging oxygen's (NBOs) [19].

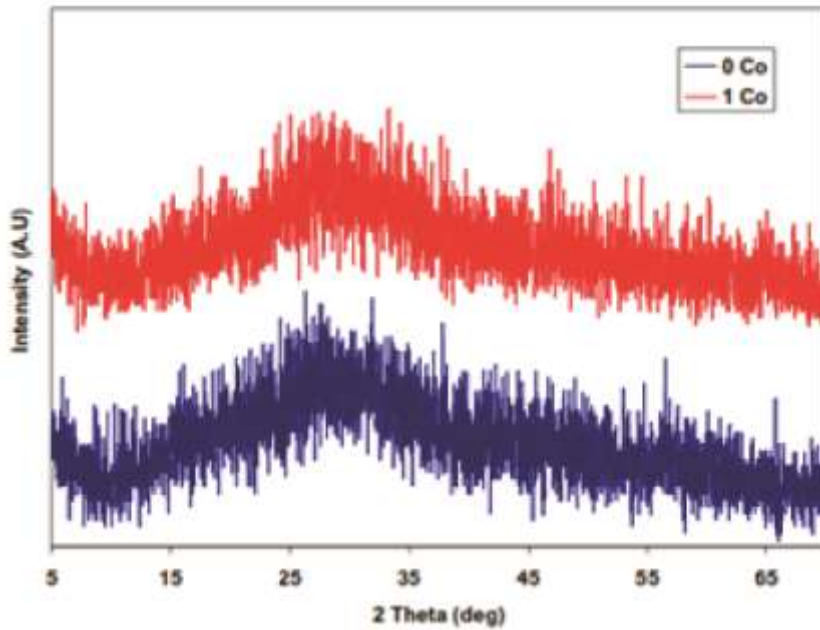


Fig. (1): X-ray diffraction patterns of Co^{2+} doped and undoped ZLB glasses.

Table [1]. Some physical properties of the glass system.

Physical quantities	Co_2O_3 mol%				
	0	0.1	0.3	0.5	1
Density, $\rho(g/cm^3)$	3.84	3.78	3.73	3.73	3.68
Molar volume, $V_m(cm^3/mol)$	30.37	30.84	31.32	31.41	31.86
Cobalt ion concentration $N(x10^{22} \text{ ions}/cm^3)$	0	1.85	5.65	9.46	19.19
Polaron radius, $r_p(A^0)$	0	1.52	1.05	0.88	0.69
Interionic distance, $r_i(A^0)$	0	3.78	2.61	2.2	1.74
E_{opt} (eV)	3.7	3.1	3.06	2.9	2.8
ΔE (eV)	0.47	0.54	0.57	0.84	0.82

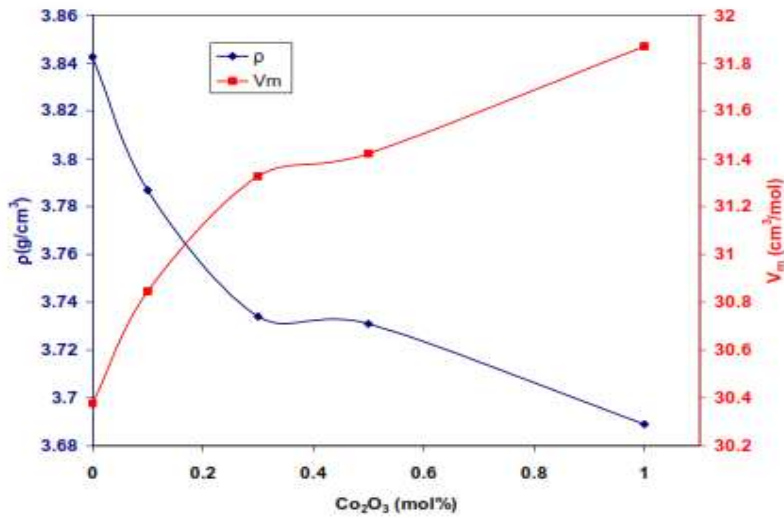


Fig. (2): Variation of the density and molar volume with Co₂O₃ concentration.

3. 2. FT-IR Spectra:

Infrared spectroscopy is usually used to obtain the essential information concerning the arrangement of the structural units of the studied glasses. It is assumed that the vibrations of structural units of the glass network are independent on the vibration of the other neighboring units [23]. The infrared absorption spectra of the ZLB glass system doped with Co₂O₃ are shown in Fig. (3). The band positions along with their assignments are given in Table (2).

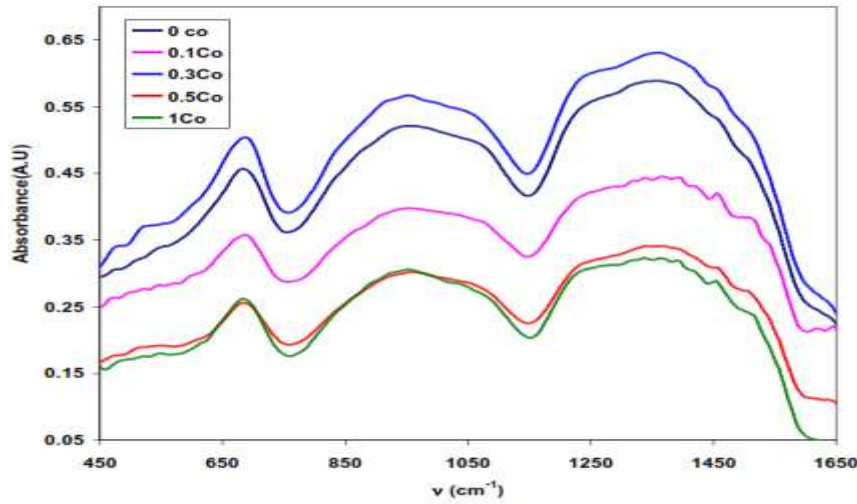


Fig. (3): IR spectra of ZLB glasses doped with different concentrations of Co_2O_3 .

Table (2): Assignment of absorption bands in the infrared spectra of the glassy system

Peak position (cm^{-1})					Assignment
0 Co	0.1 Co	0.3 Co	0.5 Co	1 Co	
615	597	580	583	591	B–O–B bending vibrations [27]
686	684	686	685	685	
872	892	817	939	864	Vibrations of NBOs in BO_4 units [30]
998	1042	944	1017	977	B–O bond stretching of BO_4 units with Pb–O bonds overlapping (950 cm^{-1}) [36,30]
1087	1089	1085	1087	1081	Vibrations of BO_4 units [30]
1222	1235	1221	1226	1220	B–O sym stretch in BO_3 units from pyro and orthoborate groups [27,35]
1375	1398	1352	1386	1376	B–O sym stretch in BO_3 units from varied types of borate groups [35,36]
1519	1528	1505	1525	1523	
1652	1650	1654	1653	1652	H–O–H bending vibrations [30]

The vibrational modes of the borate network are seen to be mainly active in the three infrared spectral regions, which are similar to those reported by several workers [24, 25]. The first group of bands, which occur at 1200-

1600 cm^{-1} , are due to the asymmetric stretching vibration of the B-O band of trigonal BO_3 units. The second group lies between 800 and 1200 cm^{-1} and is usually assigned as B-O bond stretching of the tetrahedral BO_4 units. The third group is usually observed around 680 cm^{-1} and is due to the bending vibrations of B-O-B in $[\text{BO}_3]$ trigonal [26,27]. Three broad bands are observed around 680, 900 and 1300 cm^{-1} for all investigated samples. The spectra show little changes in the center of the bands around 690, 900 and 1300 cm^{-1} and their width become broader as the Co_2O_3 content increased. The obtained broad band's may confirm the amorphous nature of the studied samples and are in agreement with X-ray measurements [28, 29]. The strongest absorption bands of the borate glass located in the range of 1230 to 1520 cm^{-1} are usually attributed to B-O symmetric stretching of $[\text{BO}_3]$ units. The absorption bands that lie in the range from 944 to 1080 cm^{-1} are assigned to B-O stretching of $[\text{BO}_4]$ units, with Pb-O bonds overlapping (950 cm^{-1}). The bands observed at 1650 cm^{-1} are attributed to H-O-H bending vibrations, which indicate that the compound contains water [30]. To get quantitative information about the structural groups in glass, the spectra have been deconvoluted. This was made by using the Spectra Manager program assuming Gaussian type function that allowed us a better identification of the absorption bands which appear in these spectra in order to perform their assignment [23]. Fig. (4), illustrated the results of the deconvolution for pure and 1 mol% Co_2O_3 doped ZLB glasses as a representatives. The obtained broad bands are a result of the overlapping of some individual bands. Each individual band has its characteristic parameters such as its center, which is related to some type of vibrations of a specific structural group, and its relative area, which is proportional to the concentration of this structural group [22]. These characteristic parameters can be used to calculate the fraction N_4 of BO_4 units in the borate matrix for each composition. N_4 can be defined as the ratio of the total of BO_4 units to the of $(\text{BO}_3+\text{BO}_4)$ units [22, 31]. From Fig. (5), it is clear that N_4 increases up to 0.3 of Co_2O_3 content, and then it decreases with increasing of Co_2O_3 content. This means that, the intensity of BO_3 units is observed to decrease, where the band due to BO_4 units is increased as cobalt oxide increases up to 0.3 mol%. Tetragonally positioned Co^{2+} ions do not induce any dangling bands but to octahedral positioned Co^{2+} ions may do so [18,32], then it decreases beyond 0.3 cobalt oxide. In compliance with the structural changes inferred from IR studies, the observed decrease in the band gap induced by the doping of Co_2O_3 concentrations, can be accounted for the changes in BO_4 and BO_3 structural units along with the increase of NBOs (with an increase of B-O- bonds). It is well known that borate glass network mixed with modifier oxides like ZnO consists of sp^2 planar BO_3 , sp^3 tetrahedral BO_4 structural

units along with non-bridging oxygen ions. Each BO₄ unit is linked to two such other units by oxygen, and the structure leads to the formation of long chain tetrahedrons. Cobalt ions are expected to exist mainly in Co²⁺ state in a glass network. However, it is quite possible for a small fraction of cobalt ions to oxidize from Co²⁺ state to Co³⁺ state during melting and annealing processes of the glasses. Co²⁺ ions occupy both octahedral and tetrahedral positions, whereas Co³⁺ ions occupy mainly octahedral positions in the glass network [18, 33].

3. 3. Optical Absorption Studies:

The optical absorption spectra of Co-doped ZLB glass systems are shown in Fig. (6). The glass samples exhibit three broad bands around 510, 570 and 630 nm in the visible region. In addition, the UV cut-off shows tendency to shift towards longer wavelengths (red shift) as the amount of Co₂O₃ content increases. The obtained broad bands are a result of the overlapping of some individual bands as shown in Fig. (7). Each individual band has its own characteristic parameters, such as its center, area and the band height; the peak positions and their corresponding assignments are given in Table (3). The occurrence of Co²⁺ in both octahedral and tetrahedral symmetry finds an explanation of the small difference between the octahedral and tetrahedral field stabilization energies. The absorption bands can be interpreted in terms of equilibrium between 6-and4-coordination Co²⁺ ions [34]. The cobalt ions are expected to exist in two viable valence states:(i) primarily Co²⁺, which occupy both the tetrahedral and octahedral coordination's with oxygen ions; (ii) Co³⁺ state with octahedral occupancy. The energy terms structure of the Co²⁺ (3d⁷) ion in tetrahedral site is similar to the energy level structure of d³ ions in octahedral site. The tetrahedral field splits the ground state into three states: ⁴T_{1g} (F) → ⁴T_{1g} (P), ⁴A_{2g} (F) and ²T_{1g} (D). Using Tanabe–Sugano diagrams for the d³ configuration, which is conjugate to (d⁷) ion, the absorption peak observed near to 570 nm is assigned to ⁴A₂(4F)→⁴T₁(4P) [35, 36].

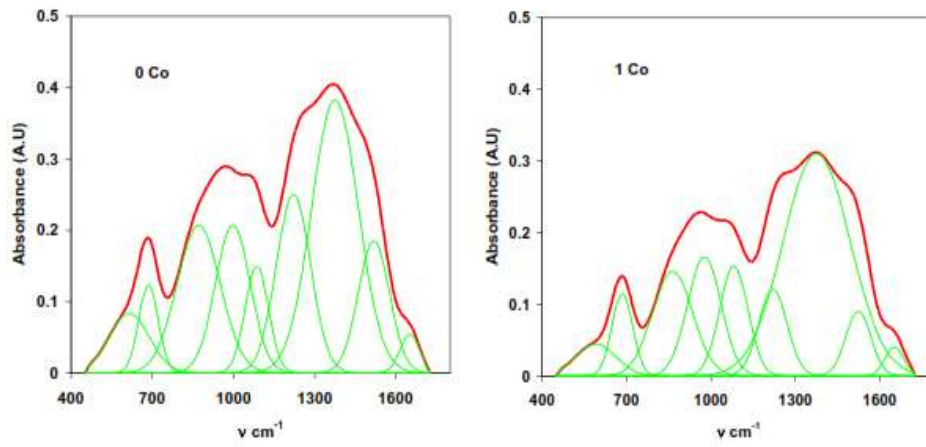


Fig. (4): Deconvoluted infrared bands for undoped ZLB glasses and doped of 1 Co²⁺.

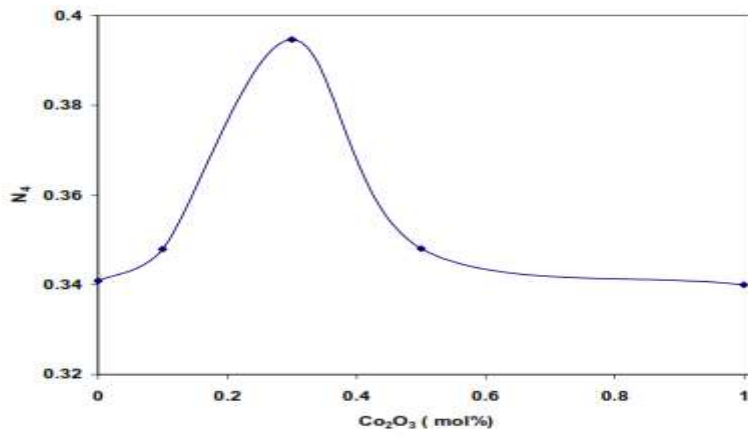


Fig. (5): The relation between N₄ and Co₂O₃ content.

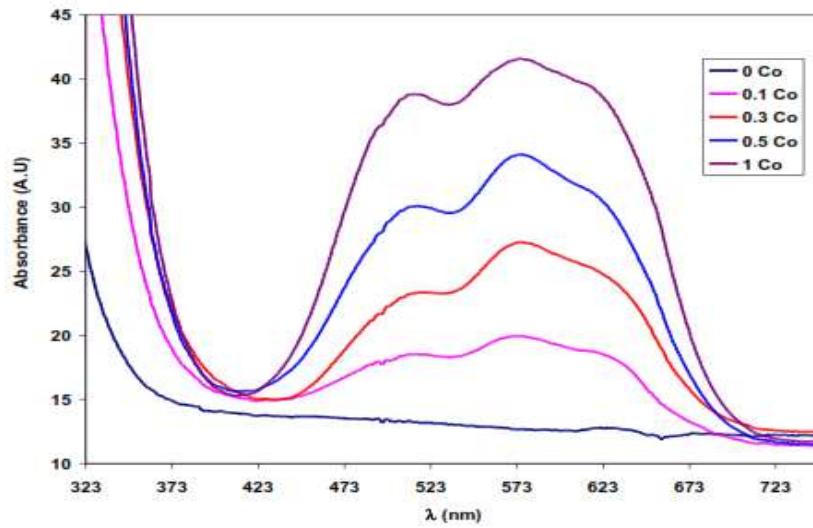


Fig. 6. Optical absorption spectra of Co^{2+} ion doped ZLB glasses.

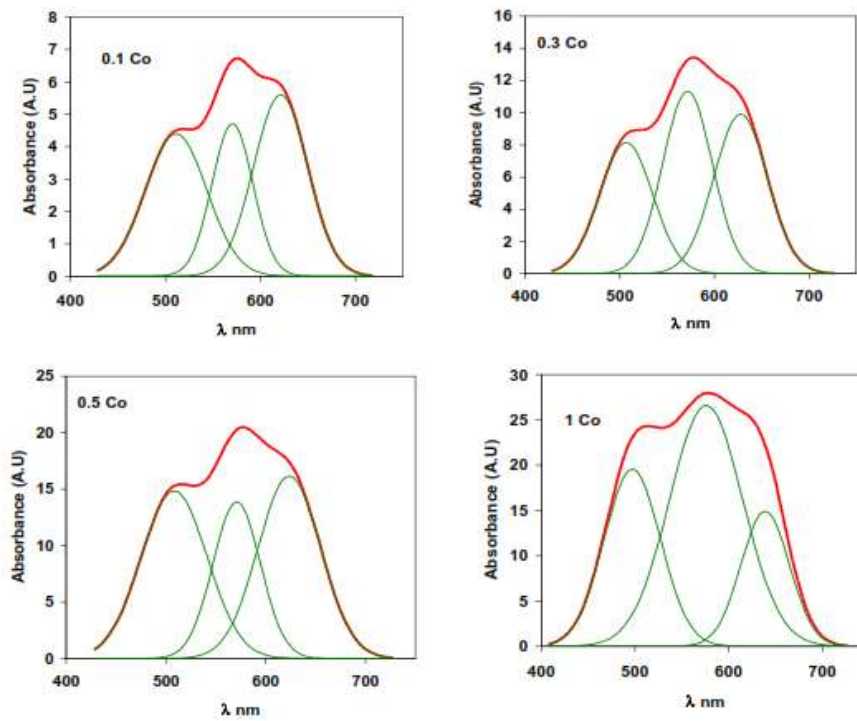


Fig. (7): Deconvoluted optical absorption bands due to ${}^4\text{T}_{1\text{g}}(\text{F})$ transition of Co^{2+} ions in ZLB glasses.

From the Table. (3) as the concentration of cobalt oxide is increased, tetrahedral positions shifted towards the shorter wavelength; such shift indicates the increase in the average distance of Co-O, whereas the octahedral band positions are shifted towards the longer wavelength with increasing intensity. The changes in the intensities of co-bands can be attributed to the changes of CoO₆ units into CoO₄ units [34]. This means that, the Co²⁺ ions are predominantly octahedrally coordinated at low Co₂O₃ content glasses, whereas in higher Co₂O₃ content glasses the Co²⁺ ions are located in tetrahedral sites. The optical absorption at the fundamental edge in terms of the theory given by Mott and Davis [37], related the absorption coefficient to the electronic energy band gap through the following relation:

$$\alpha(\omega) = B(\hbar\omega - E_g)^n/\hbar\omega \quad (4)$$

where B is a constant, E_{opt} is the optical band gap energy, and n may have the following values 2, 3, 1/2 and 1/3 depending on the inter band electronic transition.

Table (3): Peak positions, Area and Peak height of the ZLB glasses doped with Co₂O₃.

Physical parameters	Co ₂ O ₃ mol%					Assignment from
	0	0.1	0.3	0.5	1	
Peak position (nm)	-	511	507	508	498	⁴ T _{1g} (F) → ⁴ T _{1g} (P) Co ²⁺ ions
Area (arb. units)	-	357.62	572.88	1228.2	1469.4	
Peak height (arb. units)	-	4.39	8.13	14.83	19.50	
Peak position (nm)	-	570	571	571	576	⁴ A _{2g} (F) Co ²⁺ ions
Area (arb. units)	-	253.97	743.60	826.41	2612.7	
Peak height (arb. units)	-	4.70	11.32	13.85	26.54	
Peak position (nm)	-	621	628	624	639	² T _{1g} (D) Co ³⁺ ions
Area (arb. units)	-	398.69	701.18	1271.0	962.99	
Peak height (arb. units)	-	5.59	9.89	16.14	14.882	

These values of n can be understood in the framework of the ligand field theory. The data reveal that in the present case $n=2$, indicating indirect transition. This is expected since the lack of translation symmetry in non-crystalline system leads to the fact that the wave vector (momentum) is not good quantum number.

From the plot of $(\alpha\hbar\omega)^{1/n}$ versus $\hbar\omega$ (Tauc's plot), we obtain a straight line in the neighborhood of optical absorption edge. The extrapolation of the line to the energy axis with $(\alpha\hbar\omega)^{1/2} = 0$, yields the values of the optical band gap (E_{opt}), which for cobalt oxide, ZLB glasses in Fig. (8). The width of the tail of the absorption spectra can also be used to analyze possible changes in the glass structure [37]. Following the Urbach's rule [38], the optical absorption coefficient $\alpha(\omega) \approx 10^3-10^4 \text{ cm}^{-1}$, exhibits an exponential increase and is given by:

$$\alpha(\omega) = \alpha_0 \exp\left(\frac{\hbar\omega}{\Delta E}\right) \quad (5)$$

where α_0 is a constant, $\hbar\omega$ is the photon energy, and ΔE is the Urbach's energy accounting for the width of the tail of localized states. The Urbach energy (ΔE) values of the present samples were determined by taking the reciprocals of the slopes of the linear portion of the $\ln(\alpha)$ versus $\hbar\omega$ plots as shown in Fig. (9). The obtained values of E_{opt} and ΔE are listed in Table 1 and plotted in Fig. (10). We observe that E_{opt} decreases with increasing the Co_2O_3 concentration. This is likely to be related to the increase in the number of NBOs in the glass matrix, which means enhancement of the degree of disorder [35].

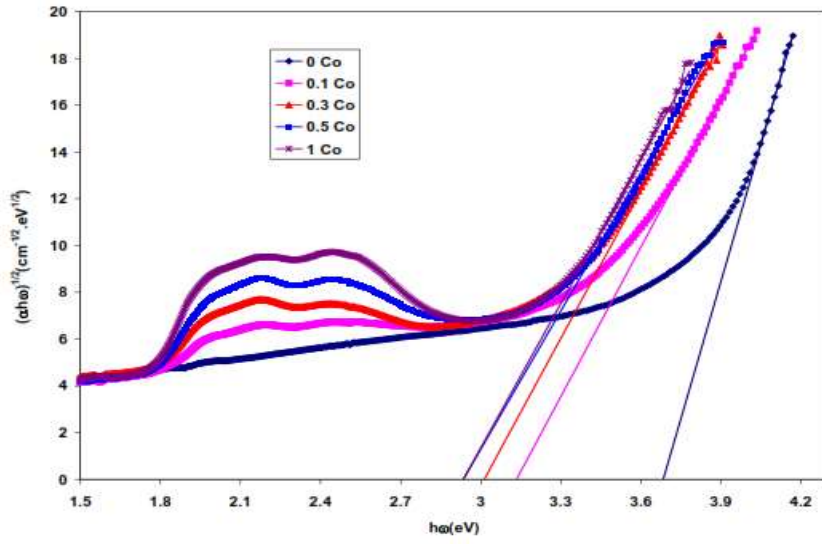


Fig. (8): Tauc's plot for Co^{1+} ions doped ZLB glasses.

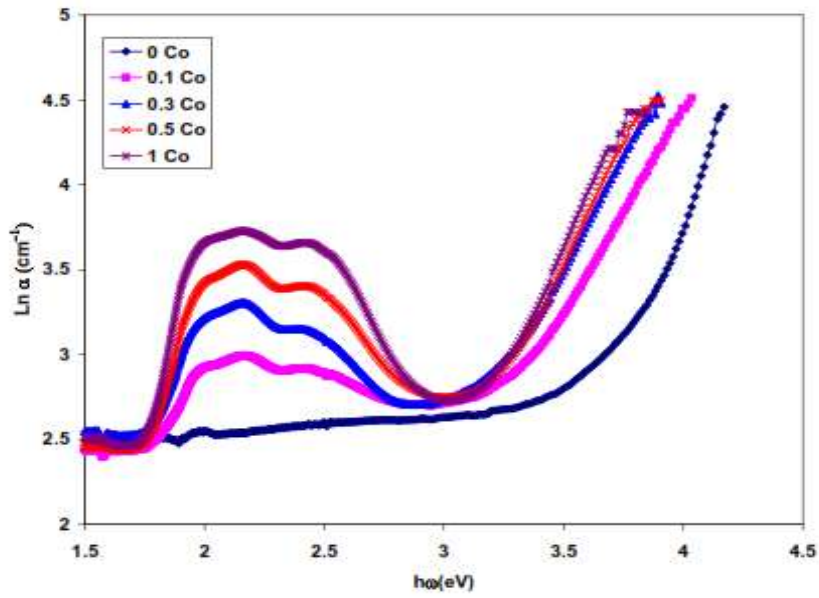


Fig. (9): Urbach plot for Co^{2+} ions doped ZLB glasses.

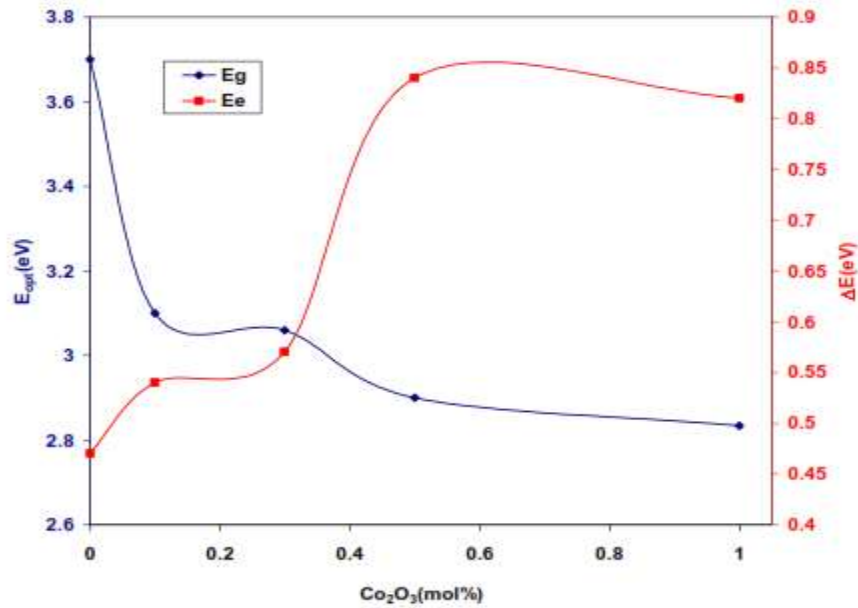


Fig. (10): Dependence of optical band gap (E_{opt}) and the Urbach's Energy (ΔE) with the Co_2O_3 concentration.

3. 4. ESR Studies:

No ESR signal is detected in the spectrum of un-doped glass. When Co^{2+} ions are introduced into the ZLB glasses, the spectra exhibit ESR signals as shown at Fig. (11). This indicates that the host glass is free from any paramagnetic centers, which means that, the observed signals are only due to Co^{2+} ions (d^7 configuration). The intensity of signals is found to increase with increasing of Co_2O_3 content. The ESR spectrum consists of a width intensity line at 3200 G, and six lines centered at 3400 G. These signals are attributed to Co^{2+} ions, which have electronic configuration $3d^7$. Therefore, Co^{2+} has $S=3/2$ and $I=7/2$. However, the observed six lines in the spectra belong to Mn^{2+} , which has the electronic configuration $3d^5$ and a total spin $S=5/2$ and $I=5/2$, This is related to the number of orientations of I with respect to external magnetic field ($m=2I+1$). That gives the usual sextet of lines in the ESR spectra in room temperature [39]. Each fine structure transition split into six hyperfine components due to the interaction of electron spin with the nucleus, having spin, $I = 7/2$. A well resolved intense signal around $g = 2.01$, characterized by weakly deformed cubic sites are observed to vary non-linearly with the concentration of Co_2O_3 , which can be attributed to near octahedral symmetry of Co^{2+} ions. The ESR parameters (the isotropic factor, g and the hyperfine splitting, A) are listed in Table (4). The increase of Co_2O_3 , up to 0.3 mol. %,

caused a decrease followed by increase of the g - and the hyperfine splitting, A , values of the glass system, respectively. Beyond this concentration, the value of g is found to increase gradually, while the value of the hyperfine splitting, A , decreases as shown in Fig. (12). The g -value for the hyperfine splitting is an indication of the nature of the bonding. If g -value shows a negative shift with respect to the free electron value (2.0023), the bonding is ionic, and if the shift is positive, the bonding is more covalent in nature. The negative value of Δg confirms the ionic bonding of glass samples, and it is observed to vary non-linearly with the increase in Co_2O_3 content [40].

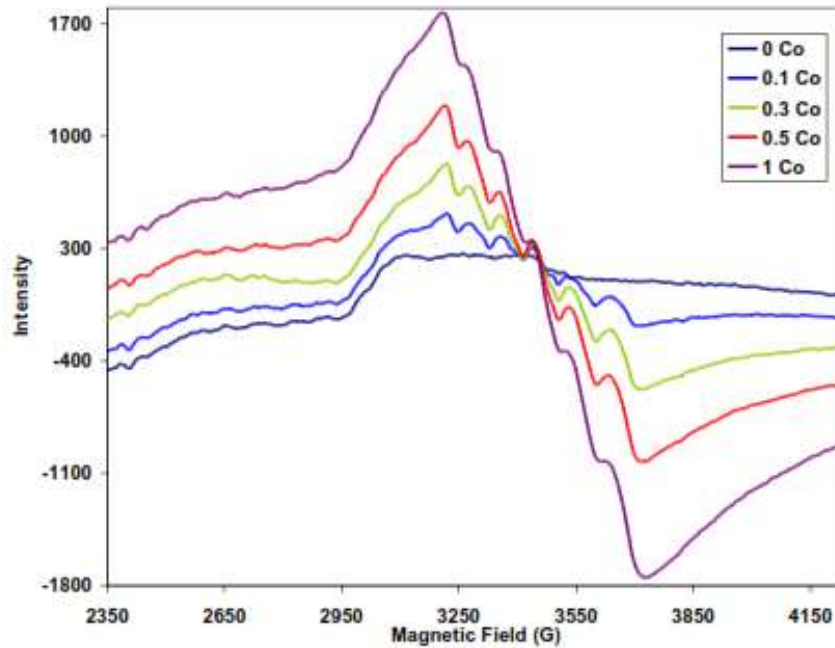


Fig. (11): ESR spectra of Co^{2+} doped zinc lead borate glass system at room

temperature.

Table (4): The spin-Hamiltonian parameters g and A for Co^{2+} ions in ZLB glasses at room temperature.

Co_2O_3 mol%	g	A (10^{-4}cm^{-1})	Δg
0	-	-	-
0.1	2.0164	82.67	-0.01413
0.3	2.0155	89.03	-0.01319
0.5	2.0164	90.62	-0.01405
1	2.0167	92.21	-0.01438

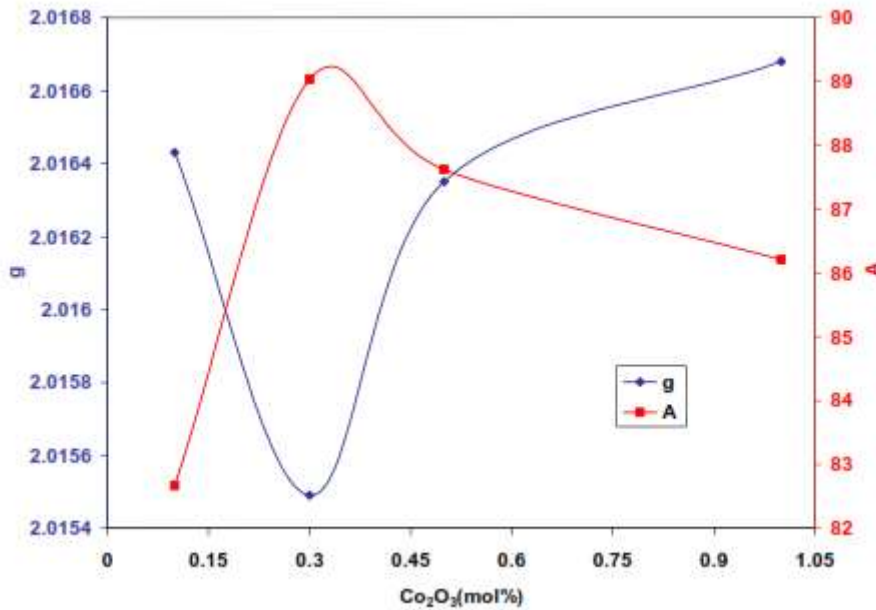


Fig. (12): Variation of g and A parameters of Co^{2+} ion doped ZLB glasses

Conclusions

The effect of Co_2O_3 concentration on structural, optical properties and ESR of ZLB glasses of composition $x\text{Co}_2\text{O}_3-(40-x)\text{ZnO}-10\text{PbO}-50\text{B}_2\text{O}_3$ are obtained spectra. It is observed that:

- 1- The glasses were prepared through melt quenching method.
- 2- The amorphous nature of the samples was confirmed through XRD analysis and the optical absorption spectra of the glasses also assure the same.
- 3- The results show that, the density and molar volume clearly depend on Co_2O_3 concentration. The molar volumes are increased with increasing of Co_2O_3 concentration, due to increase of NBOs.
- 4- The FT-IR spectra show that; all the glass samples have the BO_3 and BO_4 units and the weak band of O-H vibrations in the glassy system.
- 5- Absorption spectra of ZLB: Co^{2+} have exhibited tetrahedral and an octahedral bands.
- 6- The optical band gap decreases with increasing of Co_2O_3 . This leads to an increase in the degree of localization of electrons.

7- ESR spectra of all the glass samples showed resonance signals characteristic of Co^{2+} ions. The spin Hamiltonian parameters, g and A are found to be depended on the Co_2O_3 content. The negative value of Δg confirms the ionic bonding of glass samples, and it is varies non-linearly with the increase in Co_2O_3 content. The values of the spin Hamiltonian parameters indicate that the Co^{2+} ions in ZLB glasses present in octahedral sit with tetragonal sites.

References:

1. G. Lakshminarayana, S. Buddhudu, *Spectrochim. Acta, Part, A* **63**, **295** (2006).
2. J. Yang, S. Dai, Y. Zhou, Z.H. Jiang, *J. Appl. Phys.* **93**, 977 (2003).
3. L. Koudelka, P. Mosner, M. Zeyer, C. Jager, *J. Non-Cryst. Solids*, **326**, 72 (2003).
4. G.A. Kumar, A. Martinez, E. Mejia, C.G. Eden, *J. Alloys Compd.* **365**, 117 (2004).
5. R.V. Ravikumar, R. Komatru, K. Ikeda, A.V. chandrasekhar, B.J. Reddy, Y.P. Reddy, P.S. Rao, *J. Phys. Chem. Solids*, **64**, 261 (2003).
6. A. Thulasiramudu, S. Buddhudu, *J. Quant. Spectrosc. Radiat. Transfer*, **102**, 212 (2006).
7. A. Majchrowski, J. Ebothe, I. Fuks-Janczarek, M. Makowska-Janusik, B.Sahraoui, I. Kityk. *Opt. Mater.*, **27**, 675 (2005).
8. X. Lin-Hua, H. Ping, H. Ping *J. Phys. Chem. Solids*, **66**, 918 (2005).
9. A. Terczynska-Madej, K. Cholewalska, M. Iaczk. *Opt. Mater.*, **32**, 1456 (2010).
10. W.A. Pisarski, J. Pisarska, G. Dominiak-Dzik, W. Ryba-Romanowsk. *J. Alloys Compd.*, **484**, 45 (2009).
11. W.A. Pisarski, J. Pisarska, G. Dominiak-Dzik, M. M_łaczka, W. Ryba-omanowski, *J. Phys. Chem. Solids*, **67**, 2452 (2006).
12. B. Jamalaiah, L. Moorthy, H. Seo, *J. Non-Cryst. Solids*, **358**, 204 (2012).
13. [13] A. Speghini, M. Peruffo, M. Casarin, D. Ajo, M. Bettinelli, *J. Alloys Compd.*, **301**, 174 (2000).
14. G. Giridhar, S. Sreehari, *M. Rangacharyulu. Phys. B*, **406**, 4027 (2011).
15. G. Naga Raju, M. Srinivasa Reddy, K.S.V. Sudhakar, N. Veeraiah, *Opt. Mater.* **29**, 1467 (2007).
16. C. Lakshmikanth, B.V. Raghavaiah, N. Veeraiah, *J. Lumin.*, **109**, 190 (2004).
17. T. Raghavendra Rao, Ch. Venkata Reddy, Ch. Rama Krishna, U.S. Udayachandran Thampy, *J. Non-Cryst. Solids*, **357**, 3373 (2011).
18. P. Naresh, G. NagaRaju, Ch. SrinivasaRao, S.Prasad, V.RaviKumar,

- N. Veeraiah, *Phys. B* **407**, 712 (2012).
19. A. Uniyal, S.P. Singh, *J. Pure Appl. Phys.*, **63** (2), (2004). 109
 20. G. Laurence, C. Laurent, C. Georges, B. Valeric, *J. Non-Cryst. Solids*, **293**, 105 (2001).
 21. A.S. Rao, Y.N. Ahammed, R.R. Reddy, T.V.R. Rao, *Opt. Mater.*, **10**, 245 (1998).
 22. N. Srinivasa, M. Purnima and S. Bale, *Bull. Mater. Sci.*, **29**, 365 (2006).
 23. P. Pascuta, S. Rada, G. Borodi, M. Bosca, L. Pop, E. Culea, *J. Mol. Struct.*, **924**, 214 (2009).
 24. B. Karthikeyan, S. Mohan, *Phys.*, B **334**, 298 (2003).
 25. H. Doweidar, Y. Saddeek, *J. Non-Cryst. Solids*, **356**, 1452 (2010).
 26. S. Sindhu, S. Sanghi, A. Agarwal, V.P. Seth, N. Kishore, *Spectrochim. Acta, Part, A* **64**, 196 (2006).
 27. G. Kumari, Sk. Begum, Ch. Krishna, D. Sathisha, P. Murthy, P. Rao, R. Ravikumar, *Mater. Res. Bull.*, **47**, 2646 (2012).
 28. K. Błaszczak, A. Adamczyk, M. Wedzikowska, M. Rokita, *J. Mol. Struct.*, **704**, 275 (2004).
 29. K. Błaszczak, W. Jelonek, A. Adamczyk, *J. Mol. Struct.*, **511**, 163 (1999).
 30. T. Rao, Ch. Reddy, Ch. Krishna, U. Thampy, R. Raju, P. Rao, R. Ravikumar, *J. Non-Cryst. Solids*, **357**, 3373 (2011).
 31. S. Tanabe, *J. Alloys Compd.*, **408**, 675 (2006).
 32. M. Belkhouaja, M. Et-Tabirou, M. Elmoudane, *Phase Trans.*, **76**, 645 (2003).
 33. N.N. Greenwood, A. Earnshaw, *Chemistry of the Elements*, Butterworth-Heinemann, Oxford, UK., (1997).
 34. M. Morsi, S. El-Konsol and M. El-Shahawy, *J. non-crysta. Solids* **83**, 241 (1986).
 35. Ch. Rajyasree, A. Ramesh Babu, D. Krishna Rao, *J. Mol. Struct.*, **1033**, 200 (2013).
 36. N. Srinivasa, L. Srinivasa, Ch. Srinivasa, B. Raghavaiah, V. Ravi Kumar, *Phys. B* **407**, 581 (2012).
 37. N.F. Mott, E.A. Davis, *Philos. Mag.*, **17**, 1269 (1968).
 38. F. Urbach, *Phys. Rev.*, **92**, 1324 (1953).
 39. C. Nuhoglu, N. Demir, B. Nalbantoglu, *Tr. J. of chem.* **21**, 134 (1997).
 40. T. Raghavendra, Ch. Venkata, Ch. Ram, D. Sathish, P. Sambasiva, *Mater. Res. Bull.* **46**, 2222 (2011).